Assessment of COMSOL Capabilities to Analyse the Thermo-Hydrodynamic Behaviour of the MSR Core

A. Cammi[1], V. Di Marcello[*1], C. Fiorina[1] and L. Luzzi[1]
[1]Politecnico di Milano, Department of Energy, Nuclear Engineering Division (CeSNEF)
*Corresponding author: via Ponzio 34/3 – 20133 Milano (Italy), valentino.dimarcello@mail.polimi.it

Abstract: The present work is aimed at evaluating the capabilities of COMSOL Multiphysics® to treat heat transfer in Molten Salt Reactors (MSR). The analysed situation is represented by the molten salt in turbulent regime flowing through a cylindrical channel surrounded by graphite, with both the fluid and the solid generating power. A suitable validation framework has been set up on the basis of an ad hoc analytic solution for both velocity and temperature fields inside the fluid and the solid regions. For validation purposes, a code-to-code comparison has been also performed, using the fluid dynamics code FLUENT®.

Keywords Heat transfer, Turbulence, Molten Salt Reactor.

1. Introduction

In the last years there has been a growing interest in the Molten Salt Reactor [1], one of the six innovative concepts of fission nuclear reactors proposed in the framework of the Generation IV International Forum [2]. In this thermal-spectrum reactor, the core is composed of graphite moderator elements, each one characterized by a cylindrical channel through which a molten fluoride salt mixture containing the fissile and fertile material flows, playing the role of both fuel and coolant. As a consequence of the irradiation field, power is generated also inside the graphite, mainly due to the gamma heating. A specific feature of this reactor and, more generally, of circulating fuel systems is represented by the strong coupling between neutronics and thermo-hydrodynamics, which requires a multi-physics approach for a proper description. This approach is well offered by the COMSOL Multiphysics software [3] as witnessed by several studies performed on the subject at Politecnico di Milano [4,5,6].

Since reliable modelling of such complex and non-linear system requires qualified simulation tools, the present work is aimed at a precise assessment of COMSOL capabilities to evaluate the heat transfer and hydrodynamic pattern occurring in a typical MSR core channel. In view of the fact that scarce experimental data are available in literature, due to the uniqueness of the analysed problem, a suitable validation framework has been set up on the basis of an ad hoc analytic solution, which considers a two-dimensional domain (thanks to the axial-symmetry of the problem) and steady-state conditions. A generalized analytic approach for the heat transfer to fluids with internal heat generation, developed in a previous work at Politecnico di Milano [7], has been here extended and discussed in order to describe also the heat conduction in the graphite moderator. For completeness, a wide range of conditions has been explored, including different Reynolds and Prandtl numbers and different turbulence models. In order to get a better insight into the numerical solutions provided by COMSOL, also a code-to-code comparison has been carried out for some selected cases, adopting a dedicated computational fluid dynamics code (i.e., FLUENT® [8]).

The present work is organised as follows: in Sections 2 and 3, the physical model and its implementation in COMSOL are briefly presented; in Section 4 the analytic model used as framework for the validation purposes is described; in the last Section, the obtained results are discussed.

2. Geometry

A typical configuration of a Molten Salt Reactor core includes graphite blocks traversed by circular channels through which the power generating molten salt flows. The present work is focused on heat transfer in a single channel; hence, the analysed geometry is a smooth circular channel with constant flow section surrounded by graphite moderator.

Even if the graphite blocks can be hexagonal or square shaped, it is a good approximation to model them as a cylindrical shell. In this way, the adopted geometry is axial-symmetric and the use of a two-dimensional domain is made possible. A schematic representation of the channel and a typical mesh adopted in the present work analyses are shown in Figures 1 and 2, respectively.

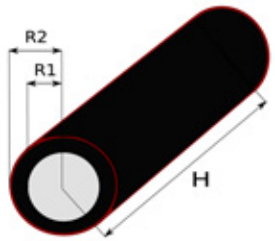

Figure 1. Adopted geometry (the graphite moderator and the molten salt are depicted in black and grey, respectively).

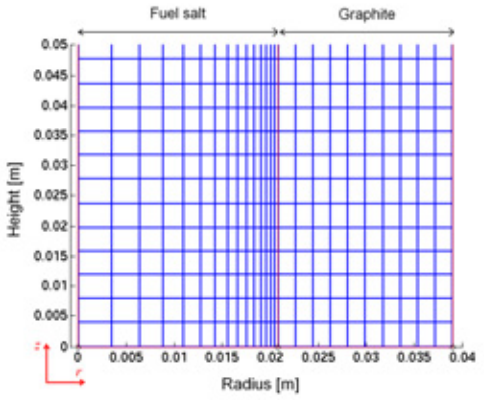

Figure 2. Mesh example of the lower part of the channel.

Throughout the paper, hydro-dynamically developed conditions are always considered. Hence the channel must be deemed as divided in two regions: in the first region the fluid becomes hydro-dynamically developed, while in the second region, the one of interest, the thermal development takes place. When the "inlet section" is mentioned, it always refers to the second region; to this region is also referred the height *H*.

3. Governing Equations and Use of COMSOL Multiphysics

As concerns the fluid motion inside the channel, the incompressible Reynolds Averaged Navier Stokes equations with Boussinesq's eddy viscosity hypothesis are adopted (see the Appendix for the meaning of symbols) [3]:

$$\nabla \bullet \boldsymbol{u} = 0 \tag{1}$$

$$\rho(\boldsymbol{u} \bullet \nabla)\boldsymbol{u} = \nabla \bullet \left[(\eta + \eta_T)(\nabla \boldsymbol{u} + (\nabla \boldsymbol{u})^T)\right] + \\ -\nabla p + \boldsymbol{F} \tag{2}$$

Temperatures can be evaluated using the energy equation:

$$\nabla \bullet \left[-(K + K_T)\nabla T\right] = Q - \rho C_p \boldsymbol{u} \bullet \nabla T \tag{3}$$

For the sake of simplicity, the physical properties of the fluid are supposed constant; hence, equations 1 and 2 do not depend on equation 3.

The turbulent conductivity K_T and the turbulent viscosity η_T take into account the enhancement of diffusivities due to turbulence. Their value can be computed using the so called "turbulence models"; in this paper the k-ε and the k-ω turbulence models are used. For brevity, only the equations governing the former are here reported:

$$\rho \boldsymbol{u} \bullet \nabla k = \nabla \bullet \left[(\eta + \frac{\eta_T}{\sigma_k})\nabla k\right] + \eta_T P(\boldsymbol{u}) - \rho\varepsilon \tag{4}$$

$$\rho \boldsymbol{u} \bullet \nabla \varepsilon = \nabla \bullet \left[(\eta + \frac{\eta_T}{\sigma_\varepsilon})\right]\nabla \varepsilon + \\ + \frac{\eta_T \varepsilon C_{\varepsilon 1} P(\boldsymbol{u})}{k} - \frac{C_{\varepsilon 2}\rho\varepsilon^2}{k} \tag{5}$$

$$P(\boldsymbol{u}) = \nabla \boldsymbol{u} : (\nabla \boldsymbol{u} + (\nabla \boldsymbol{u})^T) \tag{6}$$

$$\eta_T = \frac{\rho C_\mu k^2}{\varepsilon} \tag{7}$$

$$K_T = \frac{C_p \eta_T}{Pr_T} \tag{8}$$

where C_μ=*0.09*, $C_{\varepsilon 1}$=*1.44*, $C_{\varepsilon 2}$=*1.92*, σ_k=*1.0* and σ_ε=*1.3*. The turbulent Prandtl number (Pr_T) is obtained using the Jischa and Rieke correlation [9].

As regards the solid region, the following simple non-homogeneous diffusion equation can be adopted:

$$-\nabla \bullet (\underline{\underline{K}}^g \nabla T^g) = Q^g \tag{9}$$

As far as the boundary conditions are concerned, velocity and temperature have been imposed at the channel inlet (*z=0*), while pressure and convective flux condition have been prescribed at the outlet (*z=H*). In the lower part of the annulus, near the channel inlet, the same temperature of the fluid entering the channel has been fixed. Adiabatic conditions have been imposed in the upper part and on the external radius *R2*. On the wall between the fluid and the solid (*R1*), continuity of temperature and wall heat flux have been considered. In the analyses which do not concern the solid region (Subsection 5.1), both the conditions of imposed wall temperature and imposed wall heat flux have been used.

The governing equations of the physical model described above have been solved by means of the COMSOL software using the *Chemical Engineering* application mode; in particular, the k-ε (or k-ω) turbulence model and the *Convection and Conduction* model have been employed.

In all the COMSOL simulations of the present work, the following expression for the "thermal wall function" has been chosen [8]:

$$T^+ = Pr_T\left[\frac{1}{\kappa}ln(9.793y^+)+ \right. \\ \left. +9.24\left(\left(\frac{Pr}{Pr_T}\right)^{3/4}-1\right)\left(1+0.28e^{-0.007\frac{Pr}{Pr_T}}\right)\right] \quad (10)$$

4. The Analytic Model

The validation work has been mainly performed on the basis of ad hoc analytic solutions. In particular, two different analytic solutions have been used in order to describe velocity and temperature fields in both the fluid fuel and the graphite moderator. An overall solution has then been obtained by coupling these two analytic solutions.

4.1 Velocity and Temperature Fields inside the Channel

An analytic solution developed in a previous work [7] has been here exploited for calculating velocity and temperature fields inside the channel. The solution applies to the case of hydro-dynamically developed flow in a straight channel with smooth wall, under the following assumptions:

1. existence of a steady state;
2. incompressible fluid;
3. constant physical properties;
4. negligible axial heat conduction.

Conditions 2 and 3 allow the velocity field to be independent of the temperature one. Condition 3 also implies the absence of effects due to free convection. This condition, together with assumption 1 and the hypothesis of a hydro-dynamically developed flow, makes the *r*-component of velocity to be zero on the average. The analytic approach can be applied with boundary conditions at wall of any kind and with the presence of a volumetric heat source; besides, the boundary conditions and the heat source can be imposed with an arbitrary shape by expressing them in terms of polynomial functions.

It is worth mentioning that the generalized analytic approach developed in [7] requires the adoption of empirical correlations in order to obtain the herein so-called analytic solution used for the validation. In particular, the expressions for the turbulent Prandtl number - see equation (8) - the turbulent shear stress and the friction factor, on which the velocity profile depends, are necessary. Such correlations are supported by several experimental evidences, which ensure their validity and accuracy in a wide range of flow conditions [7].

4.2 Temperature Field in the Graphite

The temperature field inside the graphite moderator has been obtained in the case of a cylindrical shell, under the boundary conditions discussed in Section 3. As concerns the internal radius ($r=R1$), a wall temperature $T^g(R1,z)$ with whatever axial shape can be chosen. The solution has been obtained as a series of terms following a classical separation-of-variables procedure, and it is also valid for anisotropic thermal conductivity of the material; details of such procedure can be found in [10]. The obtained result is the following:

$$T^{g^*}(r,z) = \sum_n c_n \sin(\gamma_n z) F_n(r) + \phi(z) \quad (11)$$

where

$$T^{g^*}(r,z) = T^g(r,z) - T^g(r,0) \quad (12)$$

$$c_n = \frac{E_n}{F_n(R1)} \quad (13)$$

$$E_n = \frac{\int_0^H (T^{g^*}(z,R1) - \phi(z))\sin(\gamma_n z)dz}{\int_0^H \sin^2(\gamma_n z)dz} \quad (14)$$

$$F_n(r) = I_0\left(\left(\frac{K_r^g}{K_z^g}\right)^{1/2}\gamma_n r\right) + \\ + \frac{I_1\left(\left(\frac{K_r^g}{K_z^g}\right)^{1/2}\gamma_n R2\right)}{K_1\left(\left(\frac{K_r^g}{K_z^g}\right)^{1/2}\gamma_n R2\right)} K_0\left(\left(\frac{K_r^g}{K_z^g}\right)^{1/2}\gamma_n r\right) \quad (15)$$

$$\phi(z) = -\int_0^z dz' \int_0^{z'} \frac{Q^g(z'')}{K_z^g} dz'' + z \int_0^H \frac{Q^g(z')}{K_z^g} dz' \qquad (16)$$

$$\gamma_n = \frac{\pi}{2H}(2n+1) \qquad (17)$$

with n natural number.

4.3 The Overall Solution

The solution of the overall problem has been obtained by coupling the analytic solutions for the graphite and the channel. In particular, the continuity of temperature and heat flux have been imposed. It is important to remember that the analytic solution for the channel requires a boundary condition at wall in a polynomial form. The adopted procedure has been carried out by means of MATLAB® [11] on a trial and error basis through the following main steps:

- first of all, an initial value of the wall heat flux is assumed. In particular, it is supposed that all the power generated inside the graphite is transferred to the channel with an axial shape identical to that of the volumetric source in the graphite;
- the obtained heat flux is used as boundary condition for the channel;
- the temperature field inside the channel is achieved;
- the temperature field is evaluated at wall and the resulting axial profile is interpolated in the least-square sense by means of a polynomial;
- the obtained function is used as boundary condition for the graphite;
- the temperature profile inside the graphite is achieved;
- the wall heat flux is computed and the resulting axial profile is interpolated in the least-square sense by means of a polynomial;
- therefore, the procedure is repeated until convergence is eventually reached.

A source of uncertainty is certainly introduced by means of the above procedure, due to the requirement of a polynomial for the wall temperature. Moreover, the analytic solutions in both the channel and the graphite are attained as series and the numerical implementation brings with itself unavoidable errors. Anyway, the entire numerical procedure has been adjusted in order to achieve an averaged difference between graphite and channel temperatures along the wall on the order of *0.5%*. The same requirement has been imposed on the wall heat fluxes.

5. Results and Discussion

A systematic mesh sensitivity analysis has been performed in order to assure the accuracy of the obtained solutions. Therefore, the validation work has followed two fundamental steps: first, the situation inside the channel has been deeply analysed; secondly, the thermal coupling with the graphite moderator has been investigated.

The evaluation of the encountered errors has been obtained by means of the L^2 norms of the difference between the numerical and the analytic radial profiles at the channel outlet.

Four Prandtl numbers and four Reynolds numbers (in the range $Re=5 \cdot 10^3 \div 5 \cdot 10^5$) have been considered. Prandtl numbers equal to *11* and *8.8* are typically found in Molten Salt Reactors [4,6], while the values of $Pr=0.1$ and $Pr=1.0$ have been introduced for a better assessment of the COMSOL code numerical behaviour.

In the following, temperature profiles are represented in terms of temperature differences with respect to the inlet temperature (namely, $\Delta T(r,z) = T(r,z) - T_{IN}$), so that relative errors can be better appreciated graphically.

5.1 Heat Transfer inside the Channel

The analysed geometry is that of a smooth circular channel with *5 cm* radius and *3 m* height. Hydro-dynamically developed flow conditions and an internal heat generation of *200 MW/m*^{3} have been considered. Both the conditions of imposed wall heat flux and imposed wall temperature have been explored. In the former case, a *150 kW/m*^{2} uniform inward heat flux has been adopted, while in the latter case a uniform wall temperature equal to the inlet one has been chosen.

First of all, velocity profiles have been considered. The results obtained for different Reynolds numbers are reported in Table 1: it can be seen that the differences in velocity profiles are highly influenced by the Reynolds number; in particular, they become notable for very low Reynolds numbers. The profiles obtained in the case of $Re=5 \cdot 10^4$ are reported in Figure 3: the agreement is very satisfactory.

Table 1: Computational differences (%) between velocity profiles at the channel outlet resulting from COMSOL computations and analytic solutions

Re	$5\cdot10^3$	10^4	$5\cdot10^4$	$5\cdot10^5$
k-ε	10.96	8.43	3.75	1.28
k-ω	10.92	8.41	3.76	1.28

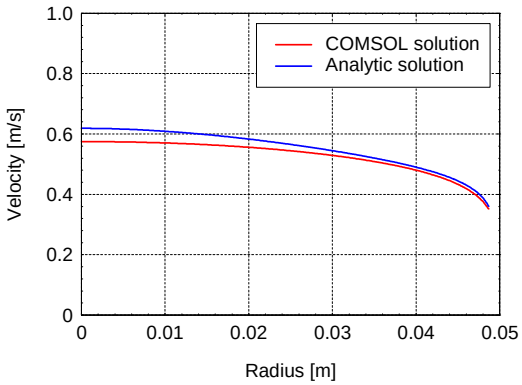

Figure 3. Velocity profiles for $Re=5\cdot10^4$.

Even better results have been obtained for temperature profiles in the case of imposed wall heat flux. The results are listed in Table 2, in which a slight dependence on the Prandtl number can be observed. Temperature profiles obtained for $Re=5\cdot10^4$ and $Pr=11$ are shown in Figure 4.

As concerns the temperature profiles in the case of imposed wall temperature, the encountered differences are reported in Table 3. The behaviour of the numerical code is absolutely satisfactory in the range of Prandtl numbers typical of Molten Salt Reactors. Such a good behaviour is confirmed in Figure 5, which depicts the profiles for $Re=5\cdot10^4$ and $Pr=11$. It can be noted from Table 3 that significant differences can be found for low Prandtl numbers. These differences are

Table 2: Imposed wall heat flux - computational differences[1] (%) between temperature radial profiles at the channel outlet resulting from COMSOL computations and analytic solutions

Re	$5\cdot10^3$ k-ε/k-ω	10^4 k-ε/k-ω	$5\cdot10^4$ k-ε/k-ω	$5\cdot10^5$ k-ε/k-ω
Pr = 11	3.84/3.80	2.71/2.69	1.77/1.77	2.11/2.15
Pr = 8.8	3.85/3.82	3.10/3.07	1.77/1.78	2.12/2.15
Pr = 1.0	4.05/4.02	2.86/2.82	1.74/1.77	2.12/2.16
Pr = 0.1	4.43/4.41	2.14/2.11	1.74/1.75	2.18/2.21

[1] Results are quoted with extra digits to better appreciate small differences.

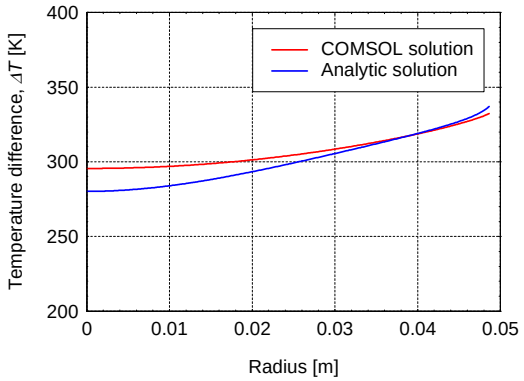

Figure 4. Imposed wall heat flux: temperature radial profiles at the channel outlet for $Re=5\cdot10^4$ and $Pr=11$.

due to the use of thermal wall functions; their presence represents indeed the main difference with respect to the case of imposed wall heat flux. Moreover, simulations have shown that the use of different wall functions can lead to quite different results. It must be pointed out that an increase of differences with decreasing Prandtl number has been also observed when internal heat generation is not considered, but the effect is less relevant.

Table 3: Imposed wall temperature - computational differences[1] (%) between temperature radial profiles at the channel outlet resulting from COMSOL computations and analytic solutions

Re	$5\cdot10^3$ k-ε/k-ω	10^4 k-ε/k-ω	$5\cdot10^4$ k-ε/k-ω	$5\cdot10^5$ k-ε/k-ω
Pr = 11	2.22/2.19	2.93/2.88	2.20/2.20	1.45/1.47
Pr = 8.8	2.19/2.15	2.70/2.64	2.23/2.23	1.46/1.47
Pr = 1.0	3.63/3.26	2.61/2.43	1.91/1.88	1.45/1.44
Pr = 0.1	30.3/30.2	20.9/20.5	10.2/10.2	2.72/2.70

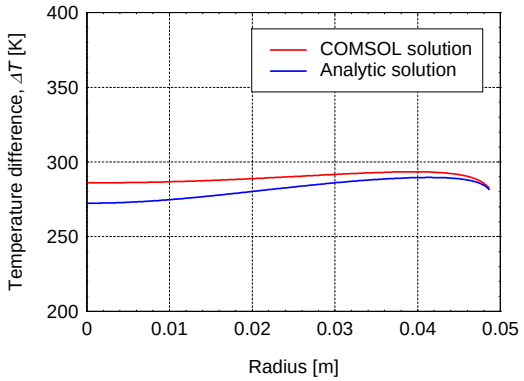

Figure 5. Imposed wall temperature: temperature radial profiles at the channel outlet for $Re=5\cdot10^4$ and $Pr=11$.

5.2 Thermal Coupling with the Graphite

In this Subsection thermal coupling between molten salt and graphite is considered and the overall solution is exploited in order to evaluate the temperature profiles. The attention is focused on the situation typical of the Molten Salt Breeder Reactor (MSBR), developed during 1970s and today still of great interest: the adopted parameters refer to the data in [12] and are listed in Table 4.

For validation purposes, analyses have been carried out also by means of the FLUENT® code. Temperature profiles at the channel outlet are reported in Figure 6. It is interesting to note that the numerical solutions tend to overestimate temperatures inside the channel; this fact is coherent with the lower velocities computed by COMSOL (Figure 3). The underestimation of temperatures inside the graphite is probably due to an underestimation of the temperature gradient at wall due to the thermal wall function. Anyway, the overall agreement can be considered acceptable from an engineering point of view. The differences encountered with respect to the analytic and FLUENT solutions are reported in Table 5: three particular locations referred to the channel outlet have been chosen, but differences of the same magnitude have been found throughout the channel and only a slight increase has been noticed approaching the inlet section.

Simulations adopting different parameters have also been performed. In particular, sinusoidal heat sources and anisotropic conductivities for the graphite have been considered. In all of these cases, results similar to those listed in Table 5 have been attained.

Table 4: Adopted parameters

Parameter	Value	Unit
H	3.96	m
$R1$	0.0208	m
$R2$	0.0390	m
Q^s	$2.135 \cdot 10^8$	W/m^3
Q^g	$2.752 \cdot 10^6$	W/m^3
v_m	1.47	m/s
ρ^s	3327	kg/m^3
K^s	1.23	W/(m·K)
η^s	0.01	Pa·s
C_p^s	1357	J/(kg·K)
K^g	31.2	W/(m·K)
Re	$2 \cdot 10^4$	-
Pr	11	-

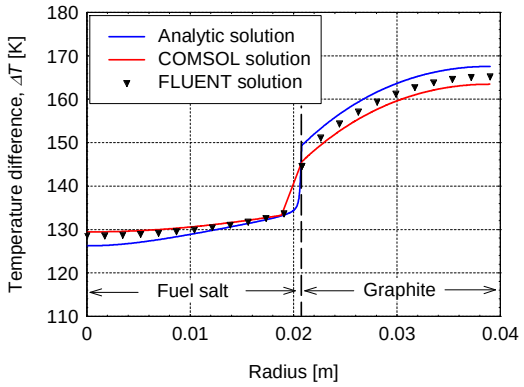

Figure 6. Temperature radial profiles at the channel outlet for $Re=2 \cdot 10^4$ and $Pr=11$.

Table 5: Computational differences (%) between temperature radial profiles at the channel outlet

	COMSOL vs. analytic solution	COMSOL vs. FLUENT solution
r = 0	2.54	0.60
r = R1	2.61	3.23
r = R2	2.45	1.13

6. Conclusions

COMSOL Multiphysics® has proved itself as a powerful tool for analysing heat transfer problems involving internal heat generation and turbulent flow, at least in the simple geometry analysed, which is representative of a typical MSR core channel. As concerns the velocity field, the numerical results are satisfactory, with notable deviations from the analytic results only for very low Reynolds numbers. Even better results have been encountered for temperature fields, but attention must be paid to the choice of the thermal wall function, which can represent an important source of errors. In this sense, equation (10) appears to be suitable when Molten Salt Reactors are under consideration. Once a suitable wall function is adopted, the behaviour of the software is satisfactory also when thermal coupling with the solid region is considered.

7. References

1. M. Hron, J. Uhlìr, C. Renault, "Molten Salt Reactor" current status and future prospects within European activities (MSR), FISA 2006 EU Research and Training in Reactor Systems, EUR 21231, 270-286 (2006)

2. A Technology Roadmap for Generation IV Nuclear Energy Systems, issued by the U.S. DOE Nuclear Energy Research Advisory Committee and the Generation IV International Forum, GIF-002-00 (2002)
3. COMSOL Multiphysics® User's Guide, version 3.5a, COMSOL AB. (2008)
4. A. Cammi, V. Di Marcello, L. Luzzi, Modelling of Circulating Nuclear Fuels with COMSOL Multiphysics, Proceedings of the European COMSOL Conference 2007, Grenoble, France, October 23-24, 380-386 (2007)
5. V. Di Marcello, A. Cammi, L. Luzzi, Analysis of coupled dynamics of molten salt reactors, Proceedings of the COMSOL Conference 2008, Hannover, Germany, November 23-24 (2008)
6. V. Di Marcello, A Multi-Physics Approach to the Modelling of the Molten Salt Reactor, Proceedings of the 2nd International Youth Conference on Energetics 2009, Budapest, Hungary, June 5 (2009)
7. V. Di Marcello, A. Cammi, L. Luzzi, A Generalized Approach to Heat Transfer in Pipe Flow with Internal Heat Generation, accepted for publication in the *Chemical Engineering Science*
8. FLUENT® User's Guide, Fluent, Inc. (2005)
9. M. Jischa, H.B. Rieke, About the prediction of turbulent Prandtl and Schmidt numbers from modified transport equations, *International Journal of Heat and Mass Transfer*, **22** (11), 1547-1555 (1979)
10. H.S. Carslaw, J.C. Jaeger, *Conduction of Heat in Solids*. Oxford University Press, London (1959)
11. MATLAB® 6.5 User's Guide, The MathWorks Inc. (2002)
12. R.C. Robertson, Conceptual design study of a single-fluid molten-salt breeder reactor, ORNL-4541 (1971)

8. Appendix

All the quantities in this work are expressed according to the International System of Units (SI) and to the nomenclature listed here below.

Latin symbols:

C_p	specific heat at constant pressure
$\boldsymbol{F}$	volume force (= **0** in this work)
k	turbulent kinetic energy
K	thermal conductivity
K_i	modified Bessel function of second kind and i-th order
K_r	radial component of thermal conductivity
K_T	turbulent thermal conductivity
K_z	axial component of thermal conductivity
$\boldsymbol{I}$	identity matrix
I_i	modified Bessel function of first kind and i-th order
p	fluid pressure
Pr	Prandtl number
Pr_T	turbulent Prandtl number
Q	volumetric heat source
r	radial coordinate
$R1$	channel radius
$R2$	graphite radius
Re	Reynolds number
T	temperature
T^+	dimensionless temperature
T_{IN}	inlet temperature of the channel
$\boldsymbol{u}$	average velocity field
v_m	mean axial velocity
y^+	dimensionless distance from the wall in the fluid region
z	axial coordinate

Greek symbols:

ΔT	temperature difference with respect to T_{IN}
ε	turbulent dissipation rate
η	dynamic viscosity
η_T	turbulent dynamic viscosity
κ	von Karman constant
ρ	density
ω	turbulent dissipation rate per unit turbulent kinetic energy

The superscript *g* is used for graphite and the superscript *s* (salt) is used for the fluid region.